

Bone Morphogenetic Protein-2 Stimulates Runx2 Acetylation*

Received for publication, November 22, 2005, and in revised form, April 5, 2006. Published, JBC Papers in Press, April 13, 2006, DOI 10.1074/jbc.M512494200

Eun-Joo Jeon[‡], Kwang-Youl Lee[‡], Nam-Sook Choi[‡], Mi-Hye Lee[§], Hyun-Nam Kim[¶], Yun-Hye Jin[‡], Hyun-Mo Ryoo[§], Je-Yong Choi[¶], Minoru Yoshida^{||}, Norikazu Nishino^{**}, Byung-Chul Oh[‡], Kyeong-Sook Lee[‡], Yong Hee Lee[‡], and Suk-Chul Bae^{‡1}

From the [‡]Department of Biochemistry, School of Medicine, and Institute for Tumor Research, Chungbuk National University, Cheongju 361-763, Korea, the [§]Department of Cell and Developmental Biology, School of Dentistry, Seoul National University, Seoul 110-749, Korea, the [¶]Department of Biochemistry, School of Medicine, Kyungpook National University, Taegu 700-422, Korea, the ^{||}Chemical Genetics Laboratory, Discovery Research Institute, RIKEN Hirosawa 2-1, Wako Saitama 351-0198, Japan, and the ^{**}Graduate School of Life Science and Systems Engineering, Kyushu Institute of Technology, 2-4, Hibikino, Wakamatsu, Kitakyushu 808-0196, Japan

Runx2/Cbfa1/PeBP2aA is a global regulator of osteogenesis and is crucial for regulating the expression of bone-specific genes. Runx2 is a major target of the bone morphogenetic protein (BMP) pathway. Genetic analysis has revealed that Runx2 is degraded through a Smurf-mediated ubiquitination pathway, and its activity is inhibited by HDAC4. Here, we demonstrate the molecular link between Smurf, HDACs and Runx2, in BMP signaling. BMP-2 signaling stimulates p300-mediated Runx2 acetylation, increasing transactivation activity and inhibiting Smurf1-mediated degradation of Runx2. HDAC4 and HDAC5 deacetylate Runx2, allowing the protein to undergo Smurf-mediated degradation. Inhibition of HDAC increases Runx2 acetylation, and potentiates BMP-2-stimulated osteoblast differentiation and increases bone formation. These results demonstrate that the level of Runx2 is controlled by a dynamic equilibrium of acetylation, deacetylation, and ubiquitination. These findings have important medical implications because BMPs and Runx2 are of tremendous interest with regard to the development of therapeutic agents against bone diseases.

Runx2/Cbfa1/PeBP2aA is a transcription factor belonging to the Runx family, which contains three members: Runx1, Runx2, and Runx3 (1). The importance of Runx proteins in mammalian development has been clearly demonstrated by gene disruption studies (2). Mouse embryos with homozygous mutations in *Runx1* showed normal morphogenesis and yolk sac-derived primitive hematopoiesis, they lacked fetal liver hematopoiesis, indicating that Runx1 is required for definitive hematopoiesis (3). Runx3 functions as a tumor suppressor of gastric cancer. *Runx3*-null gastric mucosa develops hyperplasia because of the activation of proliferation and suppression of apoptosis in epithelial cells. *Runx3*-null gastric epithelial cells are less sensitive to the growth-inhibiting and apoptosis-inducing activities of transforming growth factor- β (TGF- β).² Thus, *Runx3* is a major growth regulator of gastric

epithelial cells. Previously, we showed that the extent of the Runx3 acetylation is up-regulated by the TGF- β signaling pathway and down-regulated by histone deacetylase (HDAC) activities (4).

Runx2 is a key regulator of chondroblast and osteoblast differentiation, and of bone development *in vivo* (5–7). Targeted disruption of this *Runx2* in mice resulted in a complete lack of ossification due to the maturational arrest of osteoblasts (8–10). Runx2 regulates the expression of major extracellular matrix genes (including alkaline phosphatase, osteopontin, osteocalcin, type I collagen, and type X collagen) expressed by chondroblasts and osteoblasts (5, 11). Inactivation of one allele of the *RUNX2* gene was identified as the cause of human cleidocranial dysplasia (CCD), an autosomal dominant bone disorder (12, 13). On the other hand, constitutively active mutation of *FGFR1* results in increased Runx2 expression and the premature suture closure that is the hallmark of human craniosynostosis (14).

Expression and activation of Runx2 is regulated by many bone-derived growth factors, including bone morphogenetic proteins (BMPs) (5, 15). BMPs form a unique group of proteins within the TGF- β superfamily of genes, and play pivotal roles in the regulation of heart, neural, cartilage, and bone development (16, 17). The Smad family of proteins has been identified as the downstream propagators of BMP signals (18). BMP-activated Smads (Smad1, -5, and -8) induce *Runx2* gene expression (15), and Smads interact physically with the Runx2 protein to induce osteoblast differentiation (15, 19, 20).

The p300 protein functions primarily as a co-activator of transcription for a number of nuclear proteins including Runx family members (21–24) and also functions as a histone acetyl transferase (HAT) (25). Acetylation of specific lysine residues on histone tails is believed to neutralize the positive charge, and to generate a more accessible chromatin structure for transcription factors (26). p300 is also capable of acetylating a number of non-histone proteins (27). For example, E2F1 is acetylated by p300, and the acetylation is reversed by histone deacetylase-1 (HDAC1), indicating that reversible acetylation is also a mechanism for regulation of non-histone proteins (28). The increase in half-life through acetylation appears to protect the protein from ubiquitination, since acetylation and ubiquitination occur only at lysine residues (29, 30).

Protein ubiquitination at lysine residues plays a crucial role in defining substrate specificity and subsequent protein degradation by protea-

* This work was supported by the Creative Research Grant R16-2003-002-01001-0 from the Korea Science and Engineering Foundation (to S.-C. B.) and the Program for the Promotion of Fundamental Studies in Health Science of the National Institute of Biomedical Innovation, Japan (to N. N. and M. Y.). The costs of publication of this article were defrayed in part by the payment of page charges. This article must therefore be hereby marked "advertisement" in accordance with 18 U.S.C. Section 1734 solely to indicate this fact.

¹ To whom correspondence should be addressed: Dept. of Biochemistry, School of Medicine, and Institute for Tumor Research, Chungbuk National University, Cheongju 361-763, Korea. Tel.: 82-43-261-2842; Fax: 82-43-274-8705; E-mail: scbae@chungbuk.ac.kr.

² The abbreviations used are: TGF- β , transforming growth factor- β ; HDAC, histone

deacetylase; BMP, bone morphogenetic protein-2; OC, osteocalcin; siRNA, small interfering RNA; HA, hemagglutinin; Smurf1, Smad ubiquitin regulatory factor 1; TSA, Tricostatin A; ALP, alkaline phosphatase; RT, reverse transcriptase; GAPDH, glyceraldehyde-3-phosphate dehydrogenase; CMV, cytomegalovirus.

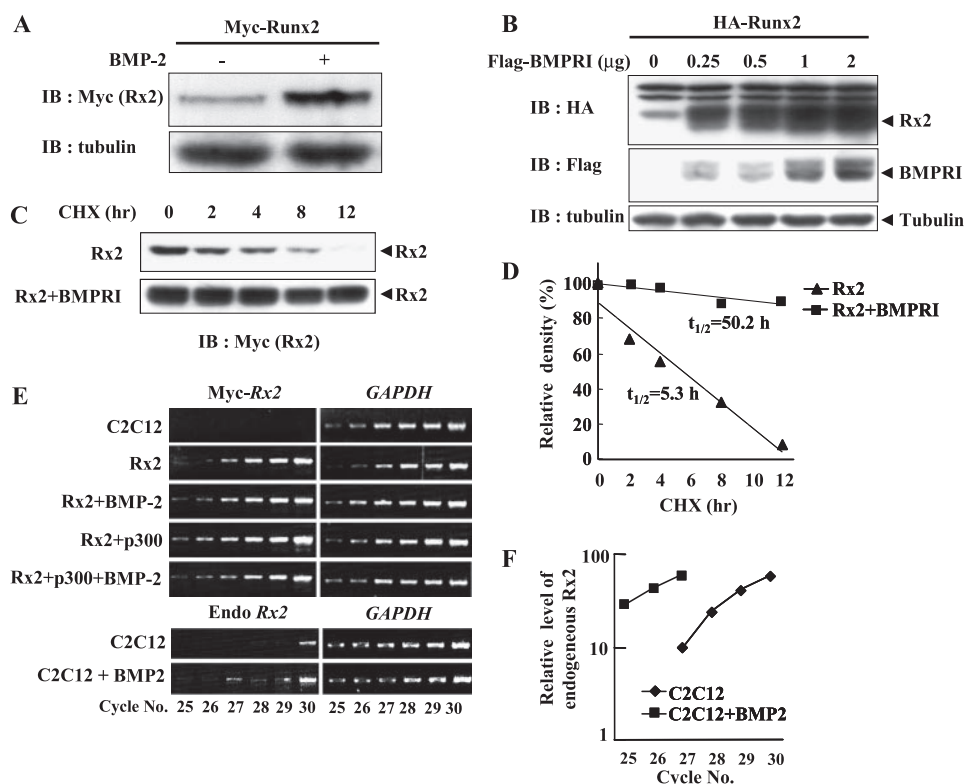


FIGURE 1. BMP-2 increases Runx2 protein levels by a transcription-independent mechanism. *A*, in C2C12 cells, Myc-tagged Runx2 was expressed in the absence (–) or presence (+) of BMP-2 (300 ng/ml). Levels of Runx2 were determined by immunoblotting (IB) using an anti-Myc antibody. *B*, in C2C12 cells, HA-tagged Runx2 was co-expressed with increasing concentrations of BMPRI. Levels of Runx2 and BMPRI were determined by immunoblotting (IB) using anti-HA and anti-FLAG antibodies, respectively. *C*, following transfection with Myc-tagged Runx2 in the presence (Rx2 + BMPRI) or absence (Rx2) of BMPRI expression, 293 cells were treated with cycloheximide (CHX, 40 μ g/ml) and cultured for the indicated times. Levels of Runx2 were determined by immunoblotting (IB) using an anti-Myc antibody. *D*, band intensities of Runx2 protein in *C* were quantitated and plotted against time to determine the half-life of Runx2 proteins in the presence (Rx2 + BMPRI) or absence (Rx2) of BMPRI expression. *E*, C2C12 cells were transfected with p300, or treated with BMP-2, and the mRNA levels of Runx2 and GAPDH were determined using semi-quantitative RT-PCR. CMV promoter-driven exogenous Runx2 mRNA and endogenous Runx2 mRNA were amplified separately. GAPDH was amplified as a control. Following RT-PCR, PCR products were collected from various reaction cycles (from 25–30), and fragments were separated using agarose gel electrophoresis. Endogenous Runx2 mRNA was amplified using forward (5'-GCTGTTAGGCCTCGTATTCTGTGA-3') and reverse (5'-CCGCTCGAGTCAATATGGC-CGCCA-3') primers. The CMV promoter-driven exogenous Runx2 mRNA was amplified with a forward primer designed against the vector sequence (5'-AGCAAGCTTGATTAGGT-GACACT-3') and a reverse primer obtained from the Runx2 coding sequence (5'-CCGCTCGAGTCTTGGTTCCCGGGACC-3'). The number of cycles performed for each PCR reaction is indicated. *F*, band intensities of endogenous Runx2 in the bottom of *E* were quantitated and plotted against the number of PCR cycles.

some. Runx2 is degraded through a ubiquitin/proteasome-mediated pathway (31, 32). Recently, Smurf1 (Smad ubiquitin regulatory factor 1) was identified as the E3 ubiquitin ligase responsible for ubiquitin-dependent Runx2 degradation (4, 33). Overexpression of Smurf1 in osteoblast precursor cells inhibits BMP signaling and osteoblast differentiation (34). Consistent with these findings, targeted inactivation of Smurf1 resulted in enhanced bone formation (35).

In contrast, *HDAC4*-null mice displayed premature ossification of developing bones, mimicking the phenotype that results from constitutive Runx2 expression. Additionally, a remarkable similarity was observed between *Runx2*-null mutants and the *HDAC4* gain-of-function phenotypes (8, 9, 36–38). A recent study demonstrated that *HDAC4* or -5 is required to inhibit Runx2 function (39), suggesting that *HDAC4* is a physiological repressor of Runx2.

Although these results clearly demonstrate that Smurf and HDAC play opposing roles in BMP signaling of Runx2 regulation, the underlying molecular links have not been clearly defined. In this study, we investigated the molecular mechanism that mediates HDAC and Smurf1 effects on Runx2. Our finding that BMP-2 induces Runx2 acetylation furnishes for the first time an important molecular link between four factors involved in osteogenesis, BMP-2, Runx2, HDAC, and Smurf1, and provides one mechanism that assembles a great deal of previously unconnected data into one coherent model.

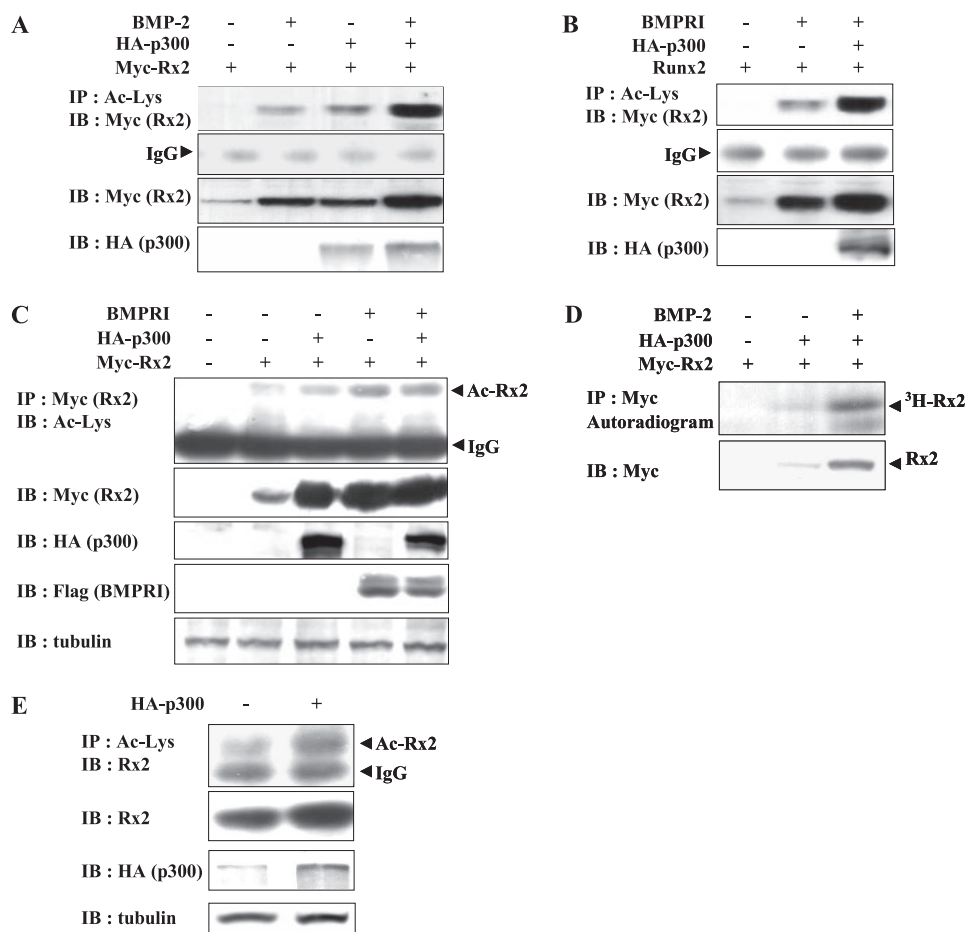
EXPERIMENTAL PROCEDURES

Cell Culture—All cell culture media and antibiotics were from Invitrogen (Carlsbad, CA). C2C12 and 293 cells were maintained in Dulbecco's modified Eagle's medium with 10% fetal bovine serum, antibiotics, and anti-mycotics, at 37 °C, in 5% CO₂. Runx2^{-/-} cell line (H1-127-21-2) was established from calvaria-like tissue of Runx2 knock-out mouse and maintained in α -MEM containing 10% fetal bovine serum, penicillin G (100 units/ml), and streptomycin (100 μ g/ml). C2C12 cells were used for the analysis, which required intact BMP signaling pathway. Runx2^{-/-} cell line was used when discrimination of Runx2-specific response from nonspecific response was required. 293 cells were used when high transfection efficiency was required and intact BMP signaling pathway was not required.

Plasmids and Antibodies—The Runx2 full-length type I isoform with MRIPV N-terminal sequence (Q08775-3) and its deletion mutants were tagged with Myc or HA, in a CMV promoter-derived mammalian expression vector (pCS4-3Myc and pCS4-3HA, respectively). Mutations affecting the Runx2 acetylation site were introduced by PCR and cloned into the pCS4-3Myc vectors. The BMP receptor 1 (BMPRI) and HA-p300 expression vectors were obtained from Dr. K. Miyazono (Tokyo University) and Dr. M. Ewen (Dana-Farber Cancer Institute, Harvard Medical School, Boston, MA), respectively. The expression plasmids for the Myc-HDAC series were cloned into pCS4-3Myc. The

BMP-2 Stimulates Runx2 Acetylation

FIGURE 2. BMP-2-mediated Runx2 stabilization is correlated with Runx2 acetylation. *A*, Myc-tagged Runx2 was expressed in C2C12 cells with BMP-2, p300, or both proteins, as indicated. Levels of acetylated Runx2 were determined by immunoprecipitation (IP) using an anti-acetyl-lysine antibody (Ac-Lys), followed by immunoblotting (IB) with an anti-Myc antibody. Runx2 (Rx2) and p300 levels were determined by immunoblotting using anti-Myc and anti-HA antibodies, respectively. *B*, Myc-tagged Runx2 was expressed in 293 cells with BMPR1, p300, or both proteins, as indicated. Levels of acetylated Runx2, Runx2 (Rx2), and p300 were determined as described above. *C*, Myc-tagged Runx2 was expressed in 293 cells with BMPR1, p300, or both proteins, as indicated. Levels of acetylated Runx2 were determined by immunoprecipitation (IP) using an anti-Myc antibody, followed by immunoblotting (IB) with an anti-acetyl-lysine antibody. Runx2 (Rx2), p300, and BMPR1 were detected by immunoblotting using anti-Myc and anti-HA antibodies, respectively. *D*, Myc-tagged Runx2 was co-expressed with p300 in 293 cells and metabolically labeled with [³H]acetate in the presence or absence of BMP-2. *Upper panel*, acetylated Runx2 was immunoprecipitated (IP) with an anti-Myc antibody and incorporation of [³H]acetate was detected by fluorography. *Lower panel*, levels of Runx2 were determined by immunoblotting (IB) using an anti-Myc antibody. *E*, C2C12 cells were transfected with vector alone or the HA-tagged p300 expression plasmid. Acetylation of endogenous Runx2 was determined by immunoprecipitation (IP) using an anti-acetyl-lysine antibody followed by immunoblotting with an anti-Runx2 antibody. Levels of endogenous Runx2 (Rx2), p300, and tubulin were determined by immunoblotting.



luciferase reporter plasmid, pGL3-T β RE, which contains two copies of TBRE (originally identified in the immunoglobulin α promoter (40)) was described previously (15). The promoter region of rat osteocalcin (−1050 OC-CAT, −1050/+23) was subcloned into the pGL2-basic vector and named pGL2−1050 OC-luc (41). The wild-type and mutated OSE2 sites (the RUNX2 binding site C of the OC promoter region (−208/+23)) have been described previously (42). In this study, antibodies against acetyl-lysine (Cell Signaling Technology, Beverly, MA), Myc (9E10, Santa Cruz Biotechnology, Santa Cruz, CA), and HA (12CA5, Roche, Basel, Switzerland) were used. The anti-Runx2 monoclonal antibody (Runx2−865) was obtained by immunizing a mouse with a Runx2 polypeptide (amino acids 272–362).

DNA Transfections and Reporter Assay—Transient transfections were performed using the calcium phosphate method for 293 cells or Lipofectamine Plus reagent (Invitrogen) for the Runx2^{−/−} cell line. Luciferase assays were performed using the Luciferase Reporter Assay kit (Promega), according to the manufacturer's recommendations. The pCMV β -gal plasmid was included as an internal control to determine the efficiency of transfection.

Immunoprecipitation and Immunoblotting—Following transfection, the C2C12 and 293 cells were lysed in ice-cold MLB buffer (25 mM HEPES (pH 7.5), 150 mM NaCl, 1% Nonidet P-40, 0.25% sodium deoxycholate, 10% glycerol, 25 mM NaF, 1 mM EDTA, 1 mM Na₃VO₄, 250 μ M phenylmethylsulfonyl fluoride, 10 μ g/ml leupeptin, and 10 μ g/ml aprotinin) and cleared by centrifugation. The resulting supernatants were immunoprecipitated with the appropriate primary and secondary antibodies, and protein A- or protein G-Sepharose beads. All incubations were conducted at 4 °C. The Sepharose beads were washed extensively

and bound proteins were separated using SDS-PAGE, and then transferred to polyvinylidene difluoride membranes. The membranes were incubated with the appropriate antibodies, washed, and then incubated with horseradish peroxidase-coupled secondary antibodies. After washing, the reactive proteins were visualized with an enhanced chemiluminescence (ECL) reagent (Amersham Biosciences). For HDAC inhibitor treatments, both C2C12 and 293 cells were cultured in fresh medium for 1 day following transfection, and then treated with the inhibitors (Tricostatin A (TSA), CHAP27 [cyclo(-_LAsu(NHOH)-_DPhe-_LPhe-_DPro)] (43) and SCOP402 [cyclo(-_Lam7(S4Py)-_DTyr(Me)-_LIle-_DPro)] (44) (also called compound 7) for 16 h, at the concentrations specified in each figure. The inhibitors were kindly provided by Dr. M. Yoshida (RIKEN).

In Vivo Sodium [³H]Acetate Labeling—The 293 cells (2 × 10⁶ cells) were incubated for 90 min in 4 ml of medium containing 4 mCi of sodium [³H]acetate (3.1 Ci/mmol, PerkinElmer Life Sciences) and 50 nM Trichostatin A. The cells were lysed in MLB buffer, and the protein extract was incubated with anti-Myc antibody. The antibody complex was then precipitated with protein G-Sepharose. Precipitates were washed four times with MLB buffer, separated using SDS-PAGE, fixed, enhanced with Amplify (Amersham Biosciences), and exposed to x-ray film at −70 °C for 10 days.

Small Interfering RNA (siRNA) Transfection—One day prior to transfection, 293 cells (3 × 10⁵ cells per well) were plated in 6-well plates and grown in Dulbecco's modified Eagle's medium containing 10% fetal bovine serum in the absence of antibiotics. Cells were transfected with pCS4−3Myc-Runx2. Five hours post-transfection, a second transfection was performed with 20 μ M Smad1 siRNA and Smad5 siRNA (Invitrogen), HDAC4 siRNA, and HDAC5 siRNA (Santa Cruz Biotech-

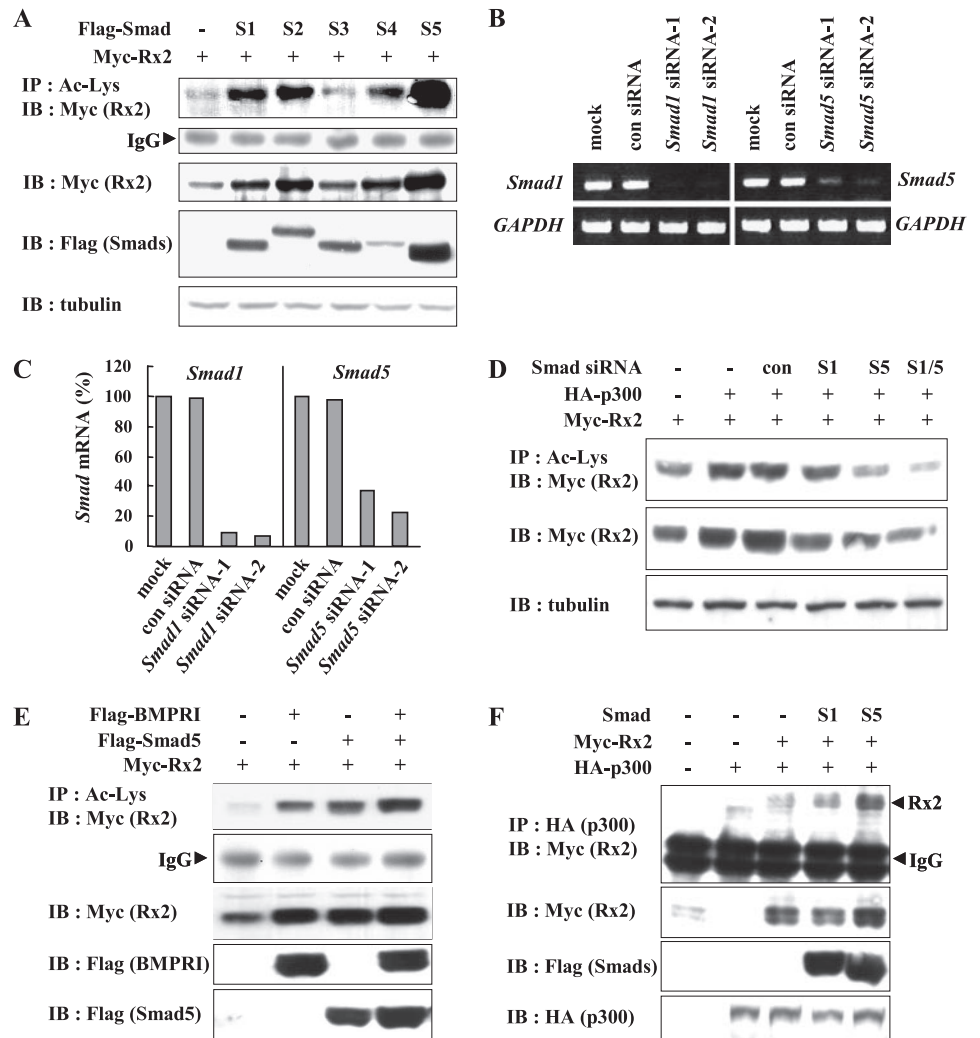


FIGURE 3. Smad is required for p300-mediated Runx2 acetylation. *A*, Myc-tagged Runx2 and various Smads were coexpressed in 293 cells, as indicated. Levels of acetylated Runx2, Runx2 (*Rx2*), and Smads were determined as described above. *B*, 293 cells were transfected with siRNAs against Smad1 or Smad5 and the mRNA levels of endogenous Smad1 and Smad5 were measured by RT-PCR. *C*, band intensities of endogenous Smad1 and Smad5 in *B* were quantitated and plotted. *D*, Myc-tagged Runx2 was co-expressed with Smad1 (*S1*) and/or Smad5 (*S5*) siRNA in 293 cells. The level of acetylated Runx2 was determined as described above. *E*, Myc-tagged Runx2 was expressed in 293 cells with BMPR1, Smad5, or both proteins, as indicated. Levels of acetylated Runx2 were determined as described above. *F*, 293 cells were transfected with Runx2, p300, Smad1 (*S1*), or Smad5 (*S5*), or the indicated combinations of these expression plasmids, and the physical interaction between Runx2 and p300 was examined by immunoprecipitation (*IP*) followed by immunoblotting (*IB*). Levels of Runx2 (*Rx2*), Smads, and p300 protein were determined by immunoblotting.

nology). pCS4-3Myc-Runx2 and siRNA were transfected using Lipofectamine and Lipofectamine2000 (Invitrogen), respectively. A commercially available nonspecific random siRNA was used as a control. Cells were harvested 48 h after the second transfection, and subjected to immunoblot analysis and RT-PCR.

Mouse Calvarial Organ Culture—Neonatal calvarial bones were obtained from 4-day-old pups of ICR mice and analysis of new bone formation was performed as described by Ref. 45. The amount of new bone formation was assessed morphologically using the Bioquant Nova Prime software (Nashville, TN).

RESULTS

BMP-2 Increases Runx2 Protein Levels via a Transcription-independent Mechanism—The pluripotent mesenchymal precursor cell line C2C12 provides a model system to study the early stage of osteoblast differentiation during bone formation. In this model, BMP-2 inhibits the differentiation of C2C12 into multinucleated myotubes and induces osteoblast differentiation (46). *Runx2* is a major target of the BMP-2 signaling pathway at the transcriptional level (15). To address whether BMP-2 regulates Runx2 post-translationally as well, C2C12 cells were transfected with Myc-tagged Runx2, in the presence or absence of BMP-2, and the protein levels were compared by immunoblotting. The level of exogenously expressed Runx2 was much higher in BMP-2-treated cells (Fig. 1A). This result was confirmed by coexpression of HA-tagged Runx2 and increasing amounts

of the BMP receptor 1 (BMPR1). Runx2 levels increased in proportion to the abundance of BMPR1 (Fig. 1B). The half-life of Runx2 was ~5.3 h in the absence of BMPR1 and extended to 50.2 h in the presence of BMPR1 (Fig. 1, C and D). To eliminate the possibility of BMP-2 mediated transcriptional activation of the transfected gene, we measured mRNA levels of exogenous and endogenous Runx2, using semi-quantitative RT-PCR. Although BMP-2 increased the level of endogenous Runx2 mRNA, the exogenous level was not affected (Fig. 1, E and F). These results suggest that, in response to BMP-2 signaling, the accumulation of exogenous Runx2 is independent of the increase in transcription, but is associated with increased stability.

BMP-2-mediated Runx2 Acetylation and Stabilization—Because Runx2 and Runx3 are degraded via the ubiquitin-proteasome-mediated pathway (4, 31, 32), and acetylation can protect proteins from ubiquitination (4, 29), we examined whether BMP-2 induces Runx2 acetylation, thereby stabilizing the Runx2 protein. Immunoblot analysis of BMP-2-transfected cells revealed that Runx2 is acetylated by BMP-2 treatment (Fig. 2A). Because p300 is associated with TGF- β superfamily signaling pathways, and Runx1 and Runx3 are targets for p300 acetyltransferase activity (4, 24, 30), we examined whether p300 is associated with BMP-2-mediated Runx2 acetylation. p300-acetylated Runx2, and p300-mediated Runx2 acetylation increased in the presence of BMP-2 (Fig. 2A, top panel). Notably, the total amount of exogenous Runx2 was proportional to acetylation levels (Fig. 2A, third panel). Similarly, overexpression of BMPR1 alone, or in combination with p300, resulted in an increase in

BMP-2 Stimulates Runx2 Acetylation

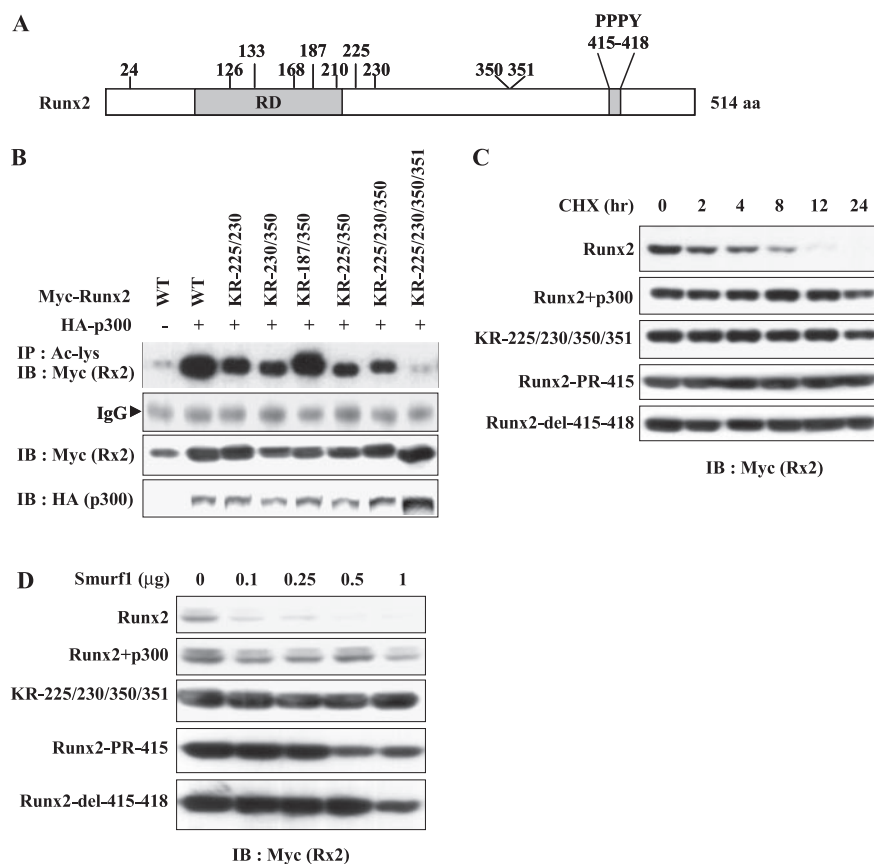


FIGURE 4. Acetylation protects Runx2 from Smurf1-mediated degradation. *A*, schematic diagram of Runx2. Numbers indicate the positions of lysine residues and the PPPY motif. All these residues are conserved among the three RUNX proteins, with the exception of Lys-350 and -351. *B*, 293 cells were transfected with plasmids expressing p300, and various Myc-tagged Runx2 mutants containing lysine to arginine (KR) substitutions. Levels of acetylated Runx2 (Ac-Rx2), Runx2 (Rx2), and p300 were determined as above. *C*, 293 cells were transfected with Myc-tagged Runx2, Runx2-KR-225/230/350/351, Runx2-PR-415, or Runx2-del-415–418, treated with cycloheximide (40 μ g/ml), and cultured for the indicated times. The transfections with Runx2 were performed in the presence or absence of p300 (0.5 μ g). The abundance of Runx2, or Runx2 mutants, was determined by immunoblotting using an anti-Myc antibody. *D*, Myc-tagged Runx2, Runx2-KR-225/230/350/351, Runx2-PR-415, or Runx2-del-415–418, were co-transfected with increasing amounts of Smurf1 as indicated in the presence or absence of p300 (0.5 μ g). Levels of expression were determined by immunoblotting using an anti-Myc antibody.

Runx2 acetylation and an accumulation of the protein (Fig. 2, *B* and *C*). Transcription of exogenous *Runx2* was unchanged by p300 and/or BMP-2 (Fig. 1*E*). Confirmation of Runx2 acetylation by p300 and BMP-2 was provided using 293 cells, in which Runx2 was metabolically labeled with [3 H]acetate. Acetylation of Runx2 increased when p300 was overexpressed and further increased in response to BMP-2 treatment (Fig. 2*D*).

To determine whether endogenous Runx2 is acetylated by p300, C2C12 cells were transfected with p300 expression plasmid and the acetylation status of Runx2 was assessed. Overexpression of p300 increased endogenous Runx2 acetylation and total Runx2 levels (Fig. 2*E*). These results demonstrate that the BMP-2 signaling pathway stimulates p300-mediated Runx2 acetylation, thereby promoting Runx2 accumulation.

Smad Is Required for p300-mediated Runx2 Acetylation—To understand how BMP-2 stimulates p300-mediated Runx2 acetylation, we transfected 293 cells with Smads and Runx2 expression plasmids and examined Runx2 acetylation. Smad2, -4, and -5 strongly increased, and Smad1 and -3 weakly increased, the level of Runx2 acetylation (Fig. 3*A*). Because Smad1 and Smad5 are known mediators of BMP-2 signaling, we examined the effect of Smad1 and Smad5 siRNA on p300-mediated Runx2 acetylation. siRNA knock-down of Smad1 and Smad5 was confirmed by RT-PCR (Fig. 3, *B* and *C*). The level of Runx2 acetylation was weakly decreased by Smad1 siRNA and strongly decreased by Smad5 siRNA. Combined Smad1 and Smad5 siRNA treatment further decreased Runx2 acetylation (Fig. 3*D*). Furthermore, coexpression of *Smad5* and *BMPRI* synergistically increased Runx2 acetylation (Fig. 3*E*), suggesting that Smads mediate Runx2 acetylation in response to BMP-2. To determine the specific role of Smads in Runx2 acetylation, *Smad1* and *Smad5* were overexpressed in 293 cells. The physical interaction between Runx2 and p300 increased when *Smad1* or *Smad5* were

overexpressed (Fig. 3*F*). Notably, Smad5 more effectively helped the interaction than Smad1. The correlation between the effect of Smad1 and Smad5 on Runx2 acetylation and the Runx2-p300 interaction suggests that BMP-2-activated Smads (mainly Smad5) stimulate p300-mediated Runx2 acetylation by facilitating the interaction between Runx2 and p300.

Acetylation Protects Runx2 from Smurf1-mediated Degradation—Runx2 contains ten lysine residues that are potential acetylation sites (Fig. 4*A*). To identify which residues are targets for acetylation, a series of *Runx2* deletion mutants were co-expressed with p300, and cell lysates were immunoprecipitated using an anti-acetyl-lysine antibody. Acetylation was detected in the central and C-terminal regions of Runx2 (data not shown). To identify the acetylated residues, various Runx2 mutants with lysine-to-arginine (KR) substitutions were examined for p300-dependent acetylation. The Runx2-KR-225/230/350/351 mutant removed virtually all Runx2 acetylation by p300 (Fig. 4*B*). Using this mutant, we examined whether acetylation is responsible for stabilization of the protein. Runx2 had a half-life of \sim 5 h, but became very stable when co-expressed with p300 (half-life $>$ 24 h) (Fig. 4*C*). In contrast, the Runx2-KR-225/230/350/351 mutant was extremely stable, even in the absence of p300 (Fig. 4*C*). These results indicate that the presence of unmodified lysine residues increases the susceptibility of the protein to degradation, and that acetylation of the lysine residues protects Runx2 from degradation.

Because Runx2 is degraded through the ubiquitin-mediated pathway and Smurf1 is the ubiquitin ligase for this pathway (33, 34), we examined whether acetylation protects Runx2 from Smurf1-mediated degradation. Runx2 was rapidly degraded when *Smurf1* is overexpressed (Fig. 4*D*). However, co-expression of *p300* counteracted the Smurf1-mediated Runx2 degradation (Fig. 4*D*). In contrast, even in the absence of

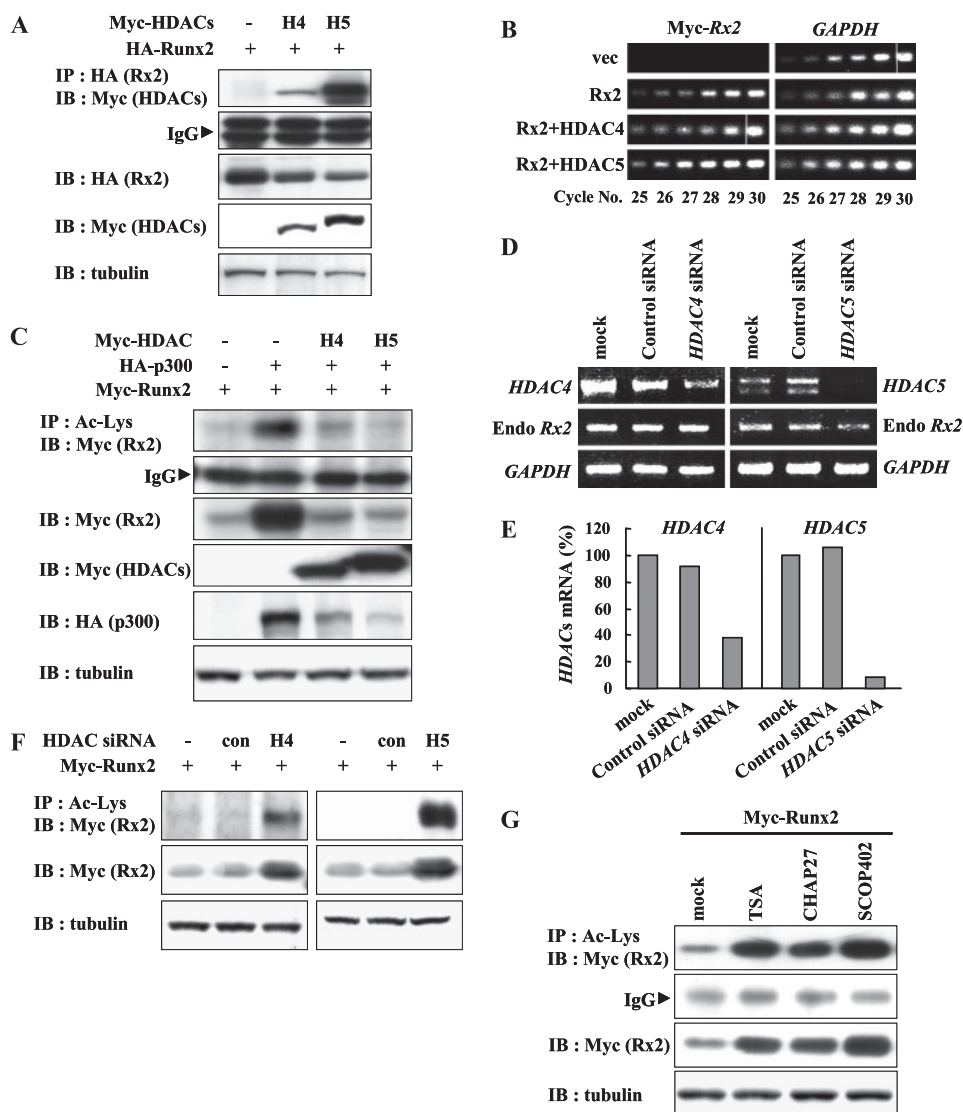


FIGURE 5. Runx2 is deacetylated by HDAC. *A*, physical interaction between Runx2 and class II HDACs. In 293 cells, HA-tagged Runx2 was coexpressed with or without Myc-tagged HDAC4 (*H4*) or HDAC5 (*H5*). The interaction between Runx2 and HDAC was analyzed by co-immunoprecipitation using an anti-HA antibody to precipitate Runx2. The abundance of Runx2 (*Rx2*) and HDACs was determined by immunoblotting using anti-HA and anti-Myc antibodies, respectively. *B*, in 293 cells, Myc-tagged Runx2 was coexpressed with HDAC4 or HDAC5 as indicated. The mRNA levels of CMV promoter-driven exogenous Runx2 and GAPDH were determined using semi-quantitative RT-PCR as described above. GAPDH was amplified as a control. Following quantitative RT-PCR, PCR products were collected from various reaction cycles (from 25–30), and fragments were separated using agarose gel electrophoresis. *C*, deacetylation of Runx2 by HDACs. In 293 cells, Myc-tagged Runx2 was co-expressed with HDAC4 (*H4*), HDAC5 (*H5*), and p300. The effect of p300 and HDACs on Runx2 acetylation and stability was analyzed by co-immunoprecipitation using an anti-acetylated-lysine antibody, and immunoblotting using an anti-Myc antibody to detect Runx2 and HDACs. Anti-tubulin was used to detect tubulin as a loading control. *D*, endogenous mRNA levels of HDAC4, HDAC5, Runx2, and GAPDH were measured by RT-PCR in HDAC4 or HDAC5 siRNA-treated cells. *E*, band intensities of endogenous HDAC4 and HDAC5 in *D* were quantitated and plotted. *F*, Myc-tagged Runx2 was co-expressed with siRNAs against HDAC4 (*H4*) or HDAC5 (*H5*) in 293 cells. The effect of HDAC4 and HDAC5 siRNA on Runx2 acetylation and protein levels were analyzed as described above. *G*, the effect of pharmacological inhibition of HDAC on Runx2. 293 cells were transfected with Myc-tagged Runx2 and treated with HDAC inhibitors (TSA, CHAP27, or SCOP402; 60 nM, 16 h). Runx2 acetylation and protein levels were analyzed as described above.

p300, the Runx2-KR-225/230/350/351 mutant was strongly resistant to Smurf1-mediated degradation.

Runx2 contains a PPXY motif that is required for interaction with the WW domain of Smurf1 (47) (Fig. 4A). To examine whether Smurf1 directly mediates Runx2 degradation, we constructed the deletion mutant Runx2-del-415–418, which lacks the PPXY motif, and the mutant Runx2-PR-415, which has a proline-to-arginine substitution at the critical amino acid 415. Both the Runx2-del-415–418 and Runx2-PR-415 mutants were extremely stable (half-life >24 h) (Fig. 4C), and were highly resistant to Smurf1-mediated degradation (Fig. 4D). These results are consistent with Smurf1-mediated degradation of Runx2.

HDAC Deacetylates Runx2—It has been shown that Runx3 acetylation is down-regulated by HDACs (4), and Runx2 activity is suppressed by class II HDACs (39) and increased by targeted inactivation of HDAC4 (37). Therefore, we examined the effect of HDAC4 and -5 on Runx2. Co-immunoprecipitation and immunoblotting analysis revealed that HDAC4 and -5 physically interacted with Runx2, and decreased Runx2 protein levels (Fig. 5A). To eliminate the possibility of HDAC-mediated transcriptional inhibition of the transfected *Runx2* gene, we measured mRNA levels of exogenous Runx2 and GAPDH, using semi-quantitative RT-PCR. The level of exogenous Runx2 mRNA was not inhibited (Fig. 5B), suggesting that the HDAC-mediated decrease of

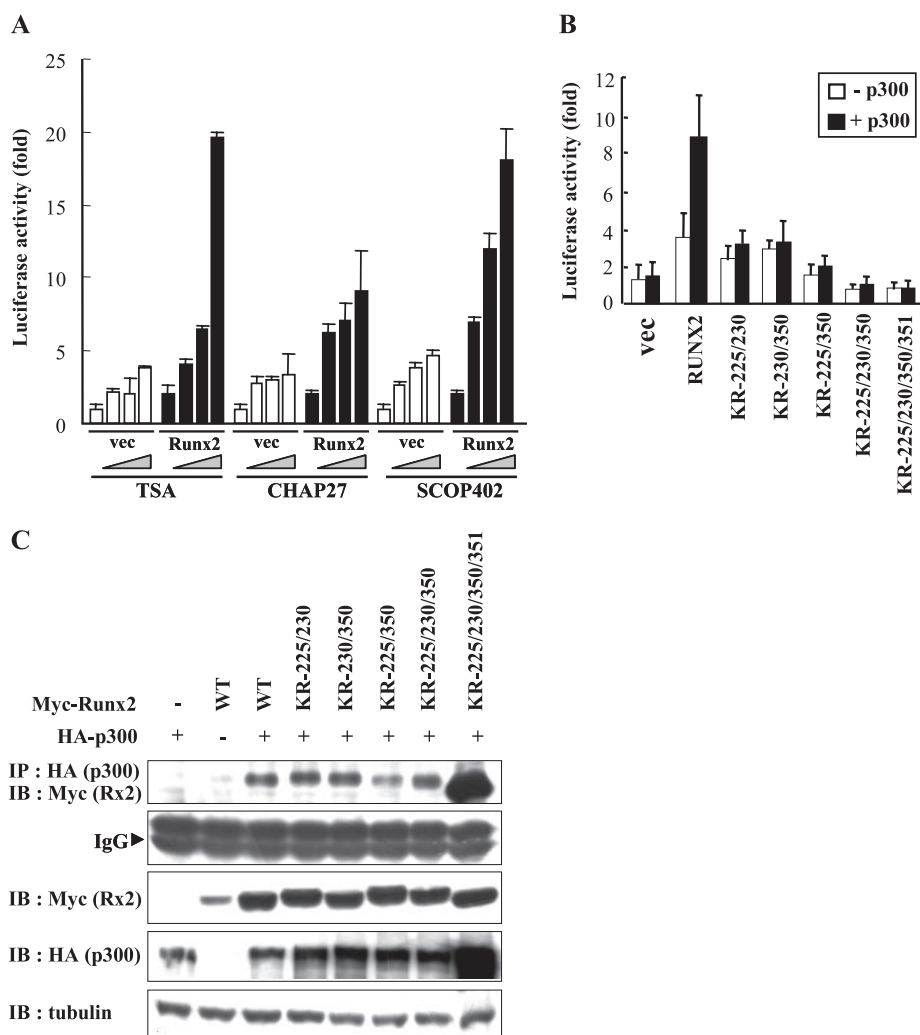
Runx2 is independent of the decrease in transcription, but is associated with the decreased protein stability. Furthermore, HDAC4 and -5 effectively decreased p300-mediated Runx2 acetylation, and Runx2 protein abundance (Fig. 5C). Consistent with this observation, siRNA-mediated knock-down of HDAC4 or -5 resulted in an increase in Runx2 acetylation, and Runx2 abundance (Fig. 5, D–F). A similar result was observed when the HDACs were inhibited by Tricostatin A (TSA), CHAP27, and SCOP402 (Fig. 5G). These results demonstrate that Runx2 acetylation/deacetylation is a dynamic process, and suggest that HDAC4 and -5 may be the effectors of Runx2 deacetylation.

Runx2 Acetylation Is Required for Its Transactivation Activity—To examine whether Runx2 acetylation affects its transactivation activity, the TGF- β responsive element-luciferase reporter plasmid (T β RE-luc) and Runx2 expression plasmids were co-transfected into 293 cells. Transfected cells were treated with increasing concentrations of HDAC inhibitors (TSA, CHAP27, or SCOP402). The HDAC inhibitors increased the Runx2-dependent reporter activity further, in a dose-dependent manner (Fig. 6A). These findings indicate that the transactivation activity of Runx2 may be increased by inhibiting Runx2 deacetylation (*i.e.* resulting in a net increase in acetylated Runx2).

To investigate whether the increase in transactivation activity of Runx2 by acetylation is a result of increased protein abundance or of the acetyla-

BMP-2 Stimulates Runx2 Acetylation

FIGURE 6. Acetylation/deacetylation controls Runx2 transactivation activity. *A*, the effect of HDAC inhibitors on Runx2-dependent transcription. 293 cells were transfected with pGL3-T β RE-luc (0.05 μ g) and the Runx2 expression plasmid (Runx2, 0.1 μ g), or empty vector (*vec*, 0.1 μ g). Transfected cells were treated with increasing concentrations of HDAC inhibitors (TSA, CHAP27, or SCOP402; 0, 30, 60, 100 nM, 16 h). The effect of HDAC inhibitors on Runx2-dependent transactivation was measured using a luciferase reporter assay. The plasmid pCMV- β gal (0.05 μ g) was included as an internal control for transfection efficiency and luciferase activities were normalized to β -galactosidase activities. Each experiment was performed in triplicate, and data from three independent experiments are presented. *B*, substitution of critical lysine residues with arginine abrogates the transactivation activity of Runx2. 293 cells were transfected with pGL3-T β RE-luc (0.05 μ g) and wild-type Runx2, or the indicated mutants in the presence or absence of co-transfected p300 expression plasmid. Runx2 transactivation activities were determined using the luciferase reporter assay as described above. *C*, 293 cells were transfected with wild-type Runx2, or the indicated mutants in the presence or absence of p300 coexpression. Interaction of Runx2 and p300 was determined by co-immunoprecipitation and protein levels of Runx2, p300, and tubulin were detected by immunoblotting.



tion itself, the transactivation activities of Runx2 and Runx2-KR mutants were measured in the presence or absence of p300. Runx2 increased luciferase reporter activity by 4-fold, relative to controls, and co-transfection with p300 increased Runx2-dependent luciferase activity by 9-fold (Fig. 6B). Notably, mutation of the lysine residues targeted by p300 caused a significant decrease in Runx2 transactivation activity (Fig. 6B), although the stability of the mutant proteins was increased (Fig. 4, B and C). Furthermore, p300 failed to increase the activity of the mutant Runx2 proteins (Fig. 6B), although the KR mutants of Runx2 still interacted with p300 (Fig. 6C). These results suggest that Runx2 acetylation is required not only for stabilization, but also for transactivation activity.

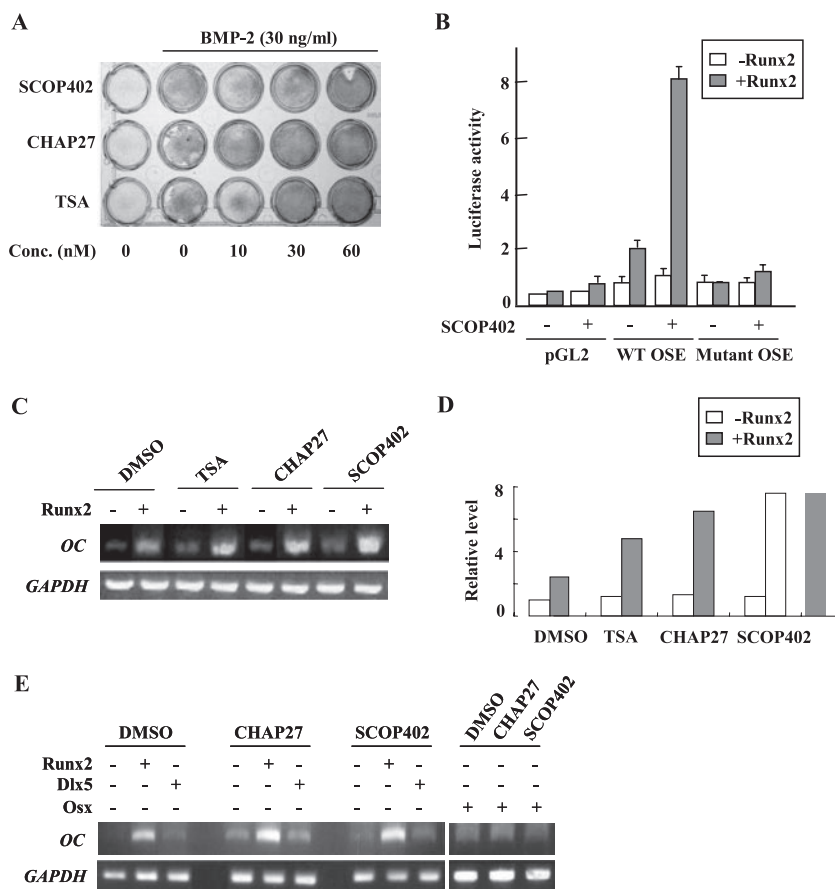
HDAC Inhibitors Stimulate Osteoblast Differentiation in Vitro—Because Runx2 is a key regulator of osteoblast differentiation, and a major target of BMP-2 signaling, we investigated whether or not HDAC inhibitors, which increase Runx2 acetylation, could also induce osteoblast differentiation. Alkaline phosphatase (ALP) is an osteoblast-specific marker that is induced in the early stages of osteoblast differentiation (46). Treatment of C2C12 pluripotent mesenchymal precursor cells with each HDAC inhibitor alone caused a slight increase in ALP activity (data not shown). The increased levels of Runx2 potentiate BMP-2 activity in osteoblast differentiation (15). Based on this observation, C2C12 cells cultured with low concentrations of BMP-2 were treated with increasing concentrations of HDAC inhibitors. BMP-2 alone (30 ng/ml, one-tenth of the usual concentration) did not increase ALP

activity. However, when combined with HDAC inhibitors, BMP-2 strongly increased ALP activity in a dose-dependent manner (Fig. 7A).

OC, another osteoblast-specific marker, is expressed at the osteoblast mineralization stage (48). To confirm that Runx2 acetylation could stimulate osteoblast differentiation, we examined the effect of HDAC inhibitors on the OC promoter and on the endogenous OC gene expression. To exclude the effects of HDAC inhibitors on endogenous Runx2, we transfected Runx2 expression plasmid and luciferase reporter plasmids in H1-127-1-2 cells, which were established from Runx2^{-/-} mouse calvaria, and treated the cells with the HDAC inhibitor, SCOP402. In the absence of Runx2, the HDAC inhibitor SCOP402 barely activated the OC promoter. Runx2 overexpression activated the OC promoter 3-fold in Runx2^{-/-} cells. In the presence of Runx2, HDAC inhibitor SCOP402 activated the OC promoter 4-fold over the activation observed for Runx2 alone (Fig. 7B). The disruption of a RUNX binding site (OSE2) in the OC promoter, completely abrogated OC promoter activation, either by HDAC inhibitor, or by Runx2 overexpression (Fig. 7B).

We examined whether or not HDAC inhibitors could affect Runx2-dependent endogenous OC gene expression. In Runx2^{-/-} cells, basal OC expression was weakly detected by RT-PCR and the treatment of HDAC inhibitors weakly stimulated basal OC expression. Transfection with Runx2 stimulated OC gene expression, and this was increased further by HDAC inhibitors (Fig. 7, C and D). A quantitative analysis of

FIGURE 7. HDAC inhibitors stimulate osteoblast differentiation. *A*, C2C12 cells were cultured for 3 days in the presence or absence of BMP-2 (30 ng/ml), and treated with increasing concentrations of HDAC inhibitors (0, 10, 30, 60 nM). Enzyme activity of the osteoblast-specific marker ALP was assayed as described by Katagiri *et al.* (46). *B*, Runx2^{-/-} cells (H1-127-21-2) were transfected with pGL2-1050 OC-luc (wild-type OSE2, WT OSE), or a RUNX binding site-mutated version (mutant OSE), with or without the Runx2 expression plasmid. The reporter activities were determined in the presence, or absence of the HDAC inhibitor SCOP402. *C*, Runx2^{-/-} cells were transfected with Runx2. After 24 h, the cells were treated with HDAC inhibitors for 3 days. RNA was then purified from the cells, and OC expression was determined by RT-PCR. The OC mRNA was amplified using forward (5'-GTGAATTCACCTAGCAGACCATGAGGAC-3') and reverse (5'-ACGGATCCGCTTCAAGCCATACTGGTCTG-3') primers. *D*, band intensities of PCR-amplified OC in *C* were quantitated and shown as a graph. *E*, Runx2^{-/-} cells were transfected with Runx2, Dlx5, or Osx expression plasmids. After 24 h, the cells were treated with HDAC inhibitors for 3 days. The levels of OC mRNA were measured by RT-PCR.



RT-PCR indicated that HDAC inhibitor-stimulated OC expression increased 3–5 times in the presence of Runx2 (Fig. 7D). This is consistent with the results of OC promoter activity analysis (Fig. 7B). Collectively, the increase in Runx2 acetylation by HDAC inhibitors strongly stimulated osteoblast differentiation.

OC Expression Is Specifically Enhanced by Runx2 Acetylation—Because OC expression can be regulated by other osteogenic transcription factors, such as Dlx5 (49), or Osterix (Osx) (50), we examined whether or not Runx2 is the specific target of HDAC inhibitors for activation of the OC promoter. The overexpression of Dlx5 or Osx weakly stimulated osteocalcin expression, and the treatment of HDAC inhibitors also weakly stimulated basal OC expression; however, the addition of HDAC inhibitors in combination of Dlx5 or Osx expression did not further stimulate OC expression in Runx2^{-/-} cells (Fig. 7E). In contrast, the combination of Runx2 overexpression and HDAC inhibitor treatment further enhanced OC mRNA expression in the cell (Fig. 7E). These results suggest that, among these three osteogenic transcription factors, Runx2 is the only target of HDAC inhibitors in osteoblast differentiation.

An HDAC Inhibitor Increases Bone Formation—We next examined the effect of HDAC inhibitors on bone formation using calvarial organ cultures from newborn mice. Simvastatin, a positive stimulator of bone formation, was used as a positive control (51). Calvaria were treated with SCOP402 or Simvastatin (Fig. 8A). The new bone areas were significantly increased in the presence of SCOP402 compared with that of vehicle-treated controls. The effect of SCOP402 is comparable to Simvastatin (51). Quantitative histomorphometric analysis is shown in Fig. 8B. These results indicate that up-regulation of Runx2 acetylation by HDAC inhibitors may not only stimulate osteoblast differentiation but also increases new bone formation.

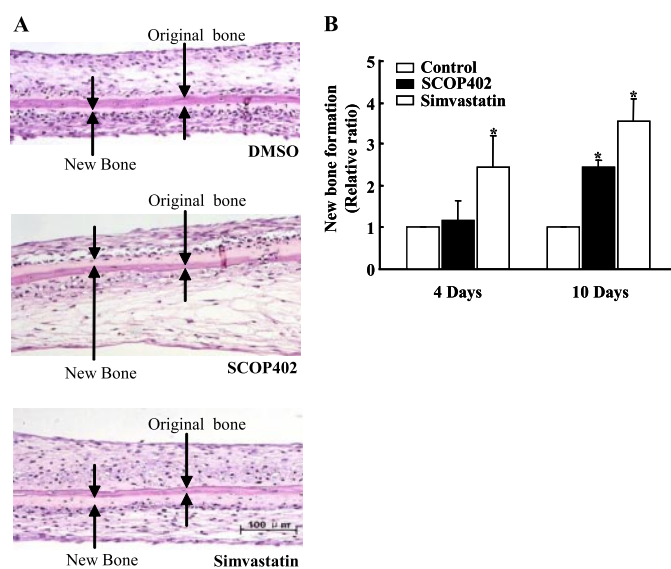


FIGURE 8. HDAC inhibitors stimulate bone formation. *A*, parietal skullcaps were explanted and cultured for 10 days with Me₂SO (0.1%), the HDAC inhibitor SCOP402 (1 μM), or Simvastatin (1 μM). Me₂SO and Simvastatin were used as the vehicle control and positive control, respectively. Sections of cultured neonatal calvarial bones were stained with hematoxylin and eosin. *B*, relative widths of new bone formation by SCOP402 and Simvastatin are shown. Bars are means ± S.E. *, *p* < 0.05 versus vehicle alone.

DISCUSSION

BMPs play pivotal roles in the regulation of bone induction, maintenance and repair. Runx2 has been identified as a master gene controlling osteoblast differentiation, and as a major target of BMP-2. BMP-2 sig-

BMP-2 Stimulates Runx2 Acetylation

naling converges on Runx2 through various pathways. First, BMP-2-activated Smads increase transcription of the *Runx2* gene (15). Secondly, BMP-2-activated Smads interact with the Runx2 protein and function synergistically to stimulate osteoblast differentiation (15, 19, 20). In this report, we demonstrate a third interaction, *i.e.* BMP-2 signaling resulting in Runx2 acetylation. Acetylation protects Runx2 from Smurf1-mediated degradation. Runx2 acetylation is mediated by the acetyltransferase activity of p300, and deacetylation is mediated by class II HDACs. Increases in acetylated Runx2 were detected when cells were treated with BMP-2 (Fig. 2), and acetylation or mutation of the lysine residues on Runx2, inhibited Smurf1-mediated Runx2 degradation (Fig. 4D). An increase in the acetylation of Runx2, via pharmacological inhibition of HDAC, potentiated BMP-2-mediated osteoblast differentiation, and increased bone formation (Figs. 7 and 8).

The acetylation of Runx2 was increased by treatment with BMP-2 and was further augmented by p300. Similarly, acetylation was increased by overexpression of BMPR1, Smads, or p300 and was further augmented by combinations of these factors. These results indicate that Runx2 acetylation is positively regulated by the BMP-2 signaling pathway, and BMP-2-activated Smads stimulate p300-mediated Runx2 acetylation by facilitating their physical interaction. However, it is unclear whether p300 is the only physiological effector of this acetylation, because P/CAF (p300- and CBP-associated factor) can also stimulate Runx2 acetylation (data not shown).

A previous report indicated that acetylation of chromatin is required for osteoblast differentiation (52). Undifferentiated cells showed low acetylation of histones H3 and H4, while differentiated osteoblasts showed higher acetylation levels. This change is coupled functionally to the chromatin remodeling events that mediate the developmental induction of osteoblast marker gene transcription, including that of OC, in bone cells (52). In this study, we suggest another function for acetylation in osteoblast differentiation. Acetylation activated the transactivation activity of Runx2, and increased its half-life, by suppressing Smurf1-mediated degradation. This enabled Runx2 to stimulate osteoblast differentiation. Our results cannot rule out the involvement of a general chromatin remodeling of osteocalcin gene promoter by histone acetylation (52) because OC expression was slightly increased by HDAC inhibitors treatment only (Fig. 7E). However, the importance of Runx2 acetylation is further supported by the results of our osteocalcin promoter activity assays, in which chromatin remodeling events were not involved (Fig. 7B). Our results also indicate that other osteogenic transcription factors, such as *Dlx5* and *Osx*, are not influenced by acetylation events (Fig. 7E).

Our data indicate that increased acetylation and abundance are both important for Runx2 activity, because mutations of the lysine residues targeted by p300 stabilized the mutant proteins, but resulted in a decrease in Runx2 transactivation activity (Fig. 6B). This result suggests that the acetylation of the lysine residues not only inhibits Smurf1-mediated ubiquitination, but also is required for transactivation activity. The addition of an acetyl group to a lysine residue could create a new surface for protein association. As the SH2 domain can interact with phospho-Tyr residues, 14-3-3 proteins can interact with phospho-Ser/Thr (53, 54), whereas the bromodomain functions as a structural module specific for acetyl lysine-containing motifs (27). Therefore, an interesting question to be addressed in the future is whether or not acetylation of Runx2 creates a new surface for protein association, thereby facilitating the binding of the protein to other cell regulatory machineries.

Previously, Vega *et al.* (37) claimed that HDAC4 inhibits Runx2 activity by blocking Runx2 DNA binding, but detailed experimental data

regarding Runx2 acetylation was not provided. However, our results clearly support a requirement for HDAC4 and -5 deacetylase activity to regulate acetylation, abundance and activity of Runx2. Moreover, several other groups have reported that HDAC inhibitors increased Runx2-dependent activation of the osteocalcin promoter (55) and osteoblast maturation and differentiation (56, 57). However, none of these reports discussed the possible acetylation/deacetylation of Runx2. Our results strongly suggest that Runx2-mediated osteogenic differentiation requires acetylation-mediated regulation of the Runx2 protein by HATs and HDACs. HDAC3 and HDAC6 have also been shown to interact with Runx2 (55, 58), suggesting that there are multiple HDACs targeting Runx2.

The proposed link between BMP-2 signaling and Runx2 acetylation is further supported by our finding that HDAC deacetylates Runx2 (Fig. 5). Treatment with HDAC inhibitors increased Runx2 acetylation (Fig. 5G), potentiated BMP-2 activity in induction of osteoblast differentiation marker (Fig. 7A) and stimulated bone formation (Fig. 8). These results strongly support our model that acetylation/deacetylation and ubiquitination are physiological mechanisms governing the abundance and activity of Runx2, which is critical for osteoblast differentiation.

Because of their osteogenic potential, BMPs and Runx2 show tremendous potential for development as therapeutic agents to heal bone fractures, prevent osteoporosis, and enhance bone formation around alloplastic materials implanted into bone. It is estimated that 100 million people worldwide are at risk for osteoporosis (59). For the treatment of osteoporosis, both inhibition of osteoclasts and activation of osteoblasts are required. Despite recent success with drugs that inhibit bone resorption, there is a clear need for osteoblast activators that will increase bone formation substantially. Mundy *et al.* (51) provided an important milestone in the development of osteoblast activators by screening chemicals that activate the *BMP-2* promoter. They found that Lovastatin and Simvastatin could induce *BMP-2* expression, thereby increasing bone formation (51). In the current study, we found that pharmacological inhibition of HDAC-dependent deacetylation enhances the osteogenic activity of BMP-2, by increasing Runx2 activity and stability. Our results provide a new theoretical basis for developing therapeutic agents against osteoporosis.

REFERENCES

1. van Wijnen, A. J., Stein, G. S., Gergen, J. P., Groner, Y., Hiebert, S. W., Ito, Y., Liu, P., Neil, J. C., Ohki, M., and Speck, N. (2004) *Oncogene* **23**, 4209–4210
2. Ito, Y. (2004) *Oncogene* **23**, 4198–4208
3. Okuda, T., van Deursen, J., Hiebert, S. W., Grosveld, G., and Downing, J. R. (1996) *Cell* **84**, 321–330
4. Jin, Y. H., Jeon, E. J., Li, Q. L., Lee, Y. H., Choi, J. K., Kim, W. J., Lee, K. Y., and Bae, S. C. (2004) *J. Biol. Chem.* **279**, 29409–29417
5. Ducy, P., Zhang, R., Geoffroy, V., Ridall, A. L., and Karsenty, G. (1997) *Cell* **89**, 747–754
6. Fujita, T., Azuma, Y., Fukuyama, R., Hattori, Y., Yoshida, C., Koida, M., Ogita, K., and Komori, T. (2004) *J. Cell Biol.* **166**, 85–95
7. Yoshida, C. A., Yamamoto, H., Fujita, T., Furuichi, T., Ito, K., Inoue, K., Yamana, K., Zanma, A., Takada, K., Ito, Y., and Komori, T. (2004) *Genes Dev.* **18**, 952–963
8. Komori, T., Yagi, H., Nomura, S., Yamaguchi, A., Sasaki, K., Deguchi, K., Shimizu, Y., Bronson, R. T., Gao, Y. H., Inada, M., Sato, M., Okamoto, R., Kitamura, Y., Yoshiki, S., and Kishimoto, T. (1997) *Cell* **89**, 755–764
9. Otto, F., Thornell, A. P., Crompton, T., Denzel, A., Gilmour, K. C., Rosewell, I. R., Stamp, G. W., Beddington, R. S., Mundlos, S., Olsen, B. R., Selby, P. B., and Owen, M. J. (1997) *Cell* **89**, 765–771
10. Choi, J. Y., Pratap, J., Javed, A., Zaidi, S. K., Xing, L., Balint, E., Dalamangas, S., Boyce, B., van Wijnen, A. J., Lian, J. B., Stein, J. L., Jones, S. N., and Stein, G. S. (2001) *Proc. Natl. Acad. Sci. U. S. A.* **98**, 8650–8655
11. Banerjee, C., McCabe, L. R., Choi, J. Y., Hiebert, S. W., Stein, J. L., Stein, G. S., and Lian, J. B. (1997) *J. Cell. Biochem.* **66**, 1–8
12. Lee, B., Thirunavukkarasu, K., Zhou, L., Pastore, L., Baldini, A., Hecht, J., Geoffroy, V., Ducy, P., and Karsenty, G. (1997) *Nat. Genet.* **16**, 307–310
13. Mundlos, S., Otto, F., Mundlos, C., Mulliken, J. B., Aylsworth, A. S., Albright, S.,

- Lindhout, D., Cole, W. G., Henn, W., Knoll, J. H., Owen, M. J., Mertelmann, R., Zabel, B. U., and Olsen, B. R. (1997) *Cell* **89**, 773–779
14. Zhou, Y. X., Xu, X., Chen, L., Li, C., Brodie, S. G., and Deng, C. X. (2000) *Hum. Mol. Genet.* **9**, 2001–2008
 15. Lee, K. S., Kim, H. J., Li, Q. L., Chi, X. Z., Ueta, C., Komori, T., Wozney, J. M., Kim, E. G., Choi, J. Y., Ryoo, H. M., and Bae, S. C. (2000) *Mol. Cell. Biol.* **20**, 8783–8792
 16. Chen, D., Zhao, M., and Mundy, G. R. (2004) *Growth Factors* **22**, 233–241
 17. Wozney, J. M., Rosen, V., Celeste, A. J., Mitscock, L. M., Whitters, M. J., Kriz, R. W., Hewick, R. M., and Wang, E. A. (1988) *Science* **242**, 1528–1534
 18. Shi, Y., and Massague, J. (2003) *Cell* **113**, 685–700
 19. Hanai, J., Chen, L. F., Kanno, T., Ohtani-Fujita, N., Kim, W. Y., Guo, W. H., Imamura, T., Ishidou, Y., Fukuchi, M., Shi, M. J., Stavnezer, J., Kawabata, M., Miyazono, K., and Ito, Y. (1999) *J. Biol. Chem.* **274**, 31577–31582
 20. Zhang, Y. W., Yasui, N., Ito, K., Huang, G., Fujii, M., Hanai, J., Nogami, H., Ochi, T., Miyazono, K., and Ito, Y. (2000) *Proc. Natl. Acad. Sci. U. S. A.* **97**, 10549–10554
 21. Lill, N. L., Grossman, S. R., Ginsberg, D., DeCaprio, J., and Livingston, D. M. (1997) *Nature* **387**, 823–827
 22. Pouponnot, C., Jayaraman, L., and Massague, J. (1998) *J. Biol. Chem.* **273**, 22865–22868
 23. Avantaggiati, M. L., Ogryzko, V., Gardner, K., Giordano, A., Levine, A. S., and Kelly, K. (1997) *Cell* **89**, 1175–1184
 24. Kitabayashi, I., Yokoyama, A., Shimizu, K., and Ohki, M. (1998) *EMBO J.* **17**, 2994–3004
 25. Ogryzko, V. V., Schiltz, R. L., Russanova, V., Howard, B. H., and Nakatani, Y. (1996) *Cell* **87**, 953–959
 26. Wolffe, A. P., and Pruss, D. (1996) *Cell* **84**, 817–819
 27. Kouzarides, T. (2000) *EMBO J.* **19**, 1176–1179
 28. Marzio, G., Wagener, C., Gutierrez, M. I., Cartwright, P., Helin, K., and Giacca, M. (2000) *J. Biol. Chem.* **275**, 10887–10892
 29. Ito, A., Kawaguchi, Y., Lai, C. H., Kovacs, J. J., Higashimoto, Y., Appella, E., and Yao, T. P. (2002) *EMBO J.* **21**, 6236–6245
 30. Gronroos, E., Hellman, U., Heldin, C. H., and Ericsson, J. (2002) *Mol. Cell.* **10**, 483–493
 31. Huang, G., Shigesada, K., Ito, K., Wee, H. J., Yokomizo, T., and Ito, Y. (2001) *EMBO J.* **20**, 723–733
 32. Tintut, Y., Parhami, F., Le, V., Karsenty, G., and Demer, L. L. (1999) *J. Biol. Chem.* **274**, 28875–28879
 33. Zhao, M., Qiao, M., Oyajobi, B. O., Mundy, G. R., and Chen, D. (2003) *J. Biol. Chem.* **278**, 27939–27944
 34. Zhao, M., Qiao, M., Harris, S. E., Oyajobi, B. O., Mundy, G. R., and Chen, D. (2004) *J. Biol. Chem.* **279**, 12854–12859
 35. Yamashita, M., Ying, S. X., Zhang, G. M., Li, C., Cheng, S. Y., Deng, C. X., and Zhang, Y. E. (2005) *Cell* **121**, 101–113
 36. Inada, M., Yasui, T., Nomura, S., Miyake, S., Deguchi, K., Himeno, M., Sato, M., Yamagiwa, H., Kimura, T., Yasui, N., Ochi, T., Endo, N., Kitamura, Y., Kishimoto, T., and Komori, T. (1999) *Dev. Dyn.* **214**, 279–290
 37. Vega, R. B., Matsuda, K., Oh, J., Barbosa, A. C., Yang, X., Meadows, E., McAnally, J., Pomajzl, C., Shelton, J. M., Richardson, J. A., Karsenty, G., and Olson, E. N. (2004) *Cell* **119**, 555–566
 38. Ueta, C., Iwamoto, M., Kanatani, N., Yoshida, C., Liu, Y., Enomoto-Iwamoto, M., Ohmori, T., Enomoto, H., Nakata, K., Takada, K., Kurisu, K., and Komori, T. (2001) *J. Cell Biol.* **153**, 87–100
 39. Kang, J. S., Alliston, T., Delston, R., and Derynck, R. (2005) *EMBO J.* **24**, 2543–2555
 40. Shi, M. J., and Stavnezer, J. (1998) *J. Immunol.* **161**, 6751–6760
 41. Lee, M. H., Javed, A., Kim, H. J., Shin, H. L., Gutierrez, S., Choi, J. Y., Rosen, V., Stein, J. L., van Wijnen, A. J., Stein, G. S., Lian, J. B., and Ryoo, H. M. (1999) *J. Cell. Biochem.* **73**, 114–125
 42. Kim, H. J., Kim, J. H., Bae, S. C., Choi, J. Y., Kim, H. J., and Ryoo, H. M. (2003) *J. Biol. Chem.* **278**, 319–326
 43. Komatsu, Y., Tomizaki, K. Y., Tsukamoto, M., Kato, T., Nishino, N., Sato, S., Yamori, T., Tsuruo, T., Furumai, R., Yoshida, M., Horinouchi, S., and Hayashi, H. (2001) *Cancer Res.* **61**, 4459–4466
 44. Nishino, N., Jose, B., Okamura, S., Ebisusaki, S., Kato, T., Sumida, Y., and Yoshida, M. (2003) *Org. Lett.* **5**, 5079–5082
 45. Garrett, I. R. (2003) *Methods Mol. Med.* **80**, 183–198
 46. Katagiri, T., Yamaguchi, A., Komaki, M., Abe, E., Takahashi, N., Ikeda, T., Rosen, V., Wozney, J. M., Fujisawa-Sehara, A., and Suda, T. (1994) *J. Cell Biol.* **127**, 1755–1766
 47. Otte, L., Wiedemann, U., Schlegel, B., Pires, J. R., Beyermann, M., Schmieder, P., Krause, G., Volkmer-Engert, R., Schneider-Mergener, J., and Oschkinat, H. (2003) *Protein Sci.* **12**, 491–500
 48. Lian, J. B., Stein, G. S., Stein, J. L., and van Wijnen, A. J. (1998) *J. Cell. Biochem. Suppl.* **30–31**, 62–72
 49. Lee, M. H., Kim, Y. J., Kim, H. J., Park, H. D., Kang, A. R., Kyung, H. M., Sung, J. H., Wozney, J. M., Kim, H. J., and Ryoo, H. M. (2003) *J. Biol. Chem.* **278**, 34387–34394
 50. Nakashima, K., Zhou, X., Kunkel, G., Zhang, Z., Deng, J. M., Behringer, R. R., and de Crombrughe, B. (2002) *Cell* **108**, 17–29
 51. Mundy, G., Garrett, R., Harris, S., Chan, J., Chen, D., Rossini, G., Boyce, B., Zhao, M., and Gutierrez, G. (1999) *Science* **286**, 1946–1949
 52. Shen, J., Hovhannissyan, H., Lian, J. B., Montecino, M. A., Stein, G. S., Stein, J. L., and Van Wijnen, A. J. (2003) *Mol. Endocrinol.* **17**, 743–756
 53. Pawson, T., and Saxton, T. M. (1999) *Cell* **97**, 675–678
 54. Yaffe, M. B. (2002) *Nat. Rev. Mol. Cell. Biol.* **3**, 177–186
 55. Schroeder, T. M., Kahler, R. A., Li, X., and Westendorf, J. J. (2004) *J. Biol. Chem.* **279**, 41998–42007
 56. Schroeder, T. M., and Westendorf, J. J. (2005) *J. Bone Miner. Res.* **20**, 2254–2263
 57. Cho, H. H., Park, H. T., Kim, Y. J., Bae, Y. C., Suh, K. T., and Jung, J. S. (2005) *J. Cell. Biochem.* **96**, 533–542
 58. Westendorf, J. J., Zaidi, S. K., Cascino, J. E., Kahler, R., van Wijnen, A. J., Lian, J. B., Yoshida, M., Stein, G. S., and Li, X. (2002) *Mol. Cell. Biol.* **22**, 7982–7992
 59. Melton, L. J., III, Johnell, O., Lau, E., Mautalen, C. A., and Seeman, E. (2004) *J. Bone Miner. Res.* **19**, 1055–1058